Electronic Supplementary Material (ESI) for Journal of Materials Chemistry A.

Supplementary Information

Competitive reactions during synthesis of zinc aluminum layered double hydroxides by thermal hydrolysis of urea

Line Boisen Staal,[a,†] Suraj Shiv Charan Pushparaj,[a] Claude Forano,[b] Vanessa Prevot,[b] Dorthe Bomholdt Ravnsbæk,[a] Morten Bjerring,[c] and Ulla Gro Nielsen,[a,*]

[a]*Department of Physics, Chemistry and Pharmacy, University of Southern Denmark, Campusvej 55, 5230 Odense M, Denmark*

[b]*Université Clermont Auvergne, CNRS, Institut de Chimie de Clermont-Ferrand, F-63000 Clermont-Ferrand, France*

[c]*Department of Chemistry and Interdisciplinary Nanoscience Center (iNANO), Gustav Wiedsvej 14, 8000 Aarhus C, Denmark*

*Corresponding author email: ugn@sdu.dk phone +456550 4401

† Current address: Department of Biology, University of Southern Denmark, Campusvej 55, 5230 Odense M, Denmark

Table of contents supporting information

Experimental details for the variations of the synthesis conditions

The following variations of the urea synthesis were attempted to optimize the LDH yield. The synthesis conditions were identical to those reported earlier [1] *except* for the modification described below and summarized in Table S1. Our reference sample is a ZnAl-LDH with nitrate as anion (U-NO_3).[1] A reduction of the total metal ion concentration results in intercalation of carbonate and a slightly higher LDH content, as reported earlier.[1]

Extended reaction time (C-110h): The reaction time was prolonged to 110 h.

Higher urea to metal content (C-Ur): The urea content was doubled.

Alternative Al reactants: Two alternative Al sources were employed instead of aluminum nitrate nonahydrate: A colloidal Al hydroxide (C-gel) and an aluminum hydroxide, $Al(OH)_3$ (C-A, Sigma-Aldrich). As a consequence, the start pH was 5.6, as these two reactants are less acidic than Al^{3+}. Colloidal aluminum was prepared by addition of 80 mL of a 0.2 M of $Al(NO_3)_3$ solution at a rate of 2mL/min to reactor, which contained 50 mL water. Simultaneously, the pH of this solution was adjusted to 5.5 by direct addition of 1 M ammonia (about 8 mL/min) to favor precipitation of colloidal aluminum hydroxide. Subsequently, $Zn(NO_3)_2$ and urea were added to freshly prepared precipitate of $Al(OH)_3$ and heated for 24 h.

Alternative Zn reactant (C-Z): ZnO (Sigma-Aldrich) was used and as a consequence, the start pH was 4.5.

Table S1: Synthesis conditions (reactants, urea:metal ratio, reaction time, and pH at end of synthesis) and the Al content determined by ICP-OES for the ZnAl-LDH samples prepared by different modifications of the urea method. The $[Zn^{2+}]$ and $[Al^{3+}]$ concentrations were 0.4 and 0.2 M, respectively.

Sample	**Zn precursor**	**Al precursor**	**[Urea] / [M]**	**Reaction time (h)**	**pH_{start}**	**pH_{end}**	**Al %**
U-NO_3	$Zn(NO_3)_2 \cdot 6H_2O$	$Al(NO_3)_3 \cdot 9H_2O$	4	24	3.1(1)	6.4(1)	42.2(1)
C-110h	$Zn(NO_3)_2 \cdot 6H_2O$	$Al(NO_3)_3 \cdot 9H_2O$	4	110	3.1(1)	8.0(1)	35.1(1)
C-Ur	$Zn(NO_3)_2 \cdot 6H_2O$	$Al(NO_3)_3 \cdot 9H_2O$	8	24	3.2(1)	8.2(1)	35.1(1)
C-gel	$Zn(NO_3)_2 \cdot 6H_2O$	Colloidal Al gel	2.5	24	5.6(1)	7.1(1)	34.2(1)
C-A	$Zn(NO_3)_2 \cdot 6H_2O$	Solid $Al(OH)_3$	4	24	5.6(1)	7.0(1)	28.2(1)
C-Z	Solid ZnO	$Al(NO_3)_3 \cdot 9H_2O$	4	24	4.5(1)	6.9(1)	32.5(1)

PXRD of the samples obtained by variation of the synthesis conditions

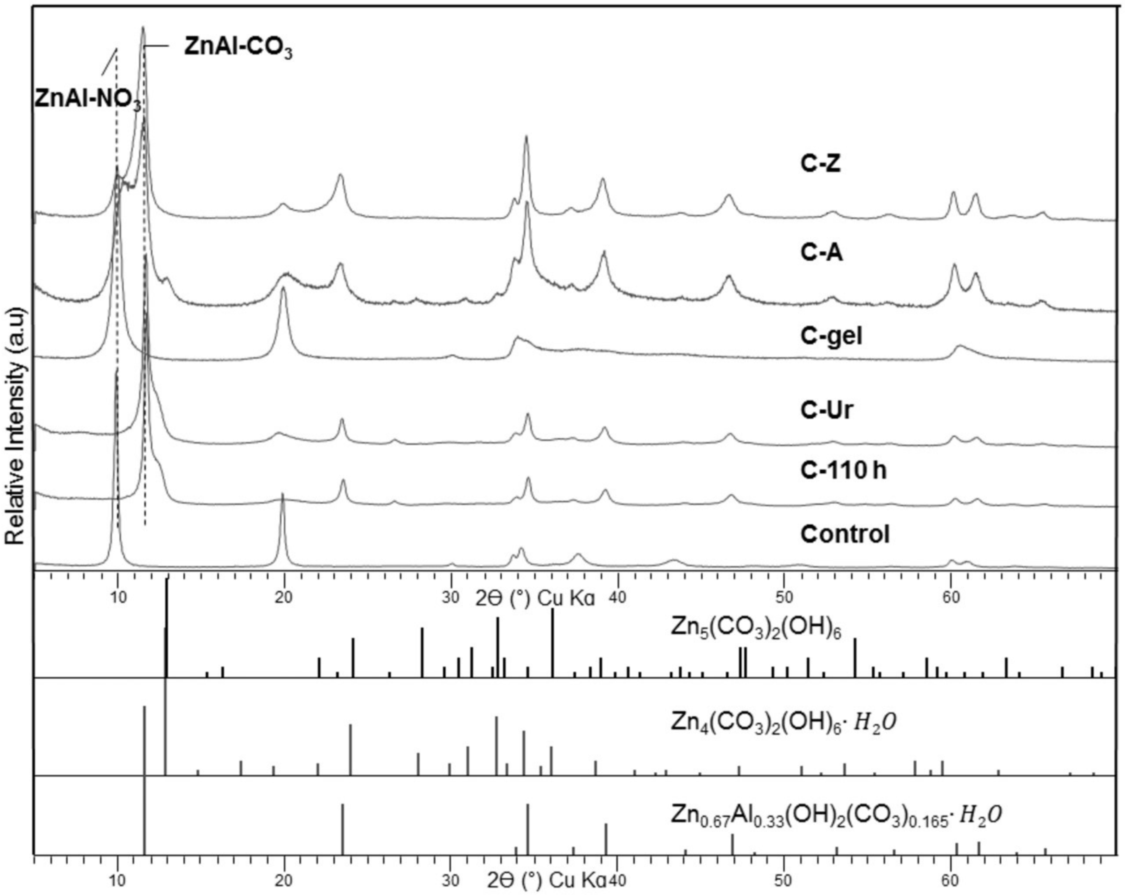

Figure S1: PXRD diffractograms of the ZnAl-LHDs C-Z, C-A, C-gel, C-UR, and C-110 as well the reference sample (U-NO_3). The samples C-110h, C-Ur, and C-A show an additional shoulder around 2θ = 12° ascribed to a layered zinc hydroxide impurity. The powder diffractograms for three reference compounds ZnAl-LDH (ICDD no. 00-048-1023) as well as two Zn-containing phases ($Zn_5(CO_3)_2(OH)_6$ (ICDD no. 00-019-1458) and $Zn_4(CO_3)_2(OH)_6 \cdot H_2O$) (ICDD no. 00-011-0287) are shown for a comparison.

Table S2: Structural identification of the second phase in ZnAl-24. The reflections for this phase as compared to Gibbsite (JCPDS-33-0018).

Gibbsite				ZnAl-24
H	**K**	**L**	**d(hkl) (Å)**	**d(hkl) (Å)**
				7.0814
				4.5383
0	0	2	4.88512	
1	1	0	4.40935	4.3918
2	0	0	4.35729	
2	0	-2	3.38766	
1	1	-2	3.34042	3.3601
1	1	2	3.20988	3.2146
				3.0145
				2.8222
3	1	-1	2.48703	
0	2	1	2.47278	2.4613
3	1	1	2.40542	
0	2	2	2.26473	
3	1	2	2.18304	
3	1	-3	2.06582	
0	2	3	2.01069	1.9995
3	1	3	1.93242	
3	1	-4	1.81946	
0	2	4	1.76589	1.7692
3	1	4	1.69833	1.6813
3	3	0	1.46978	
6	0	0	1.45243	
3	1	-6	1.41360	

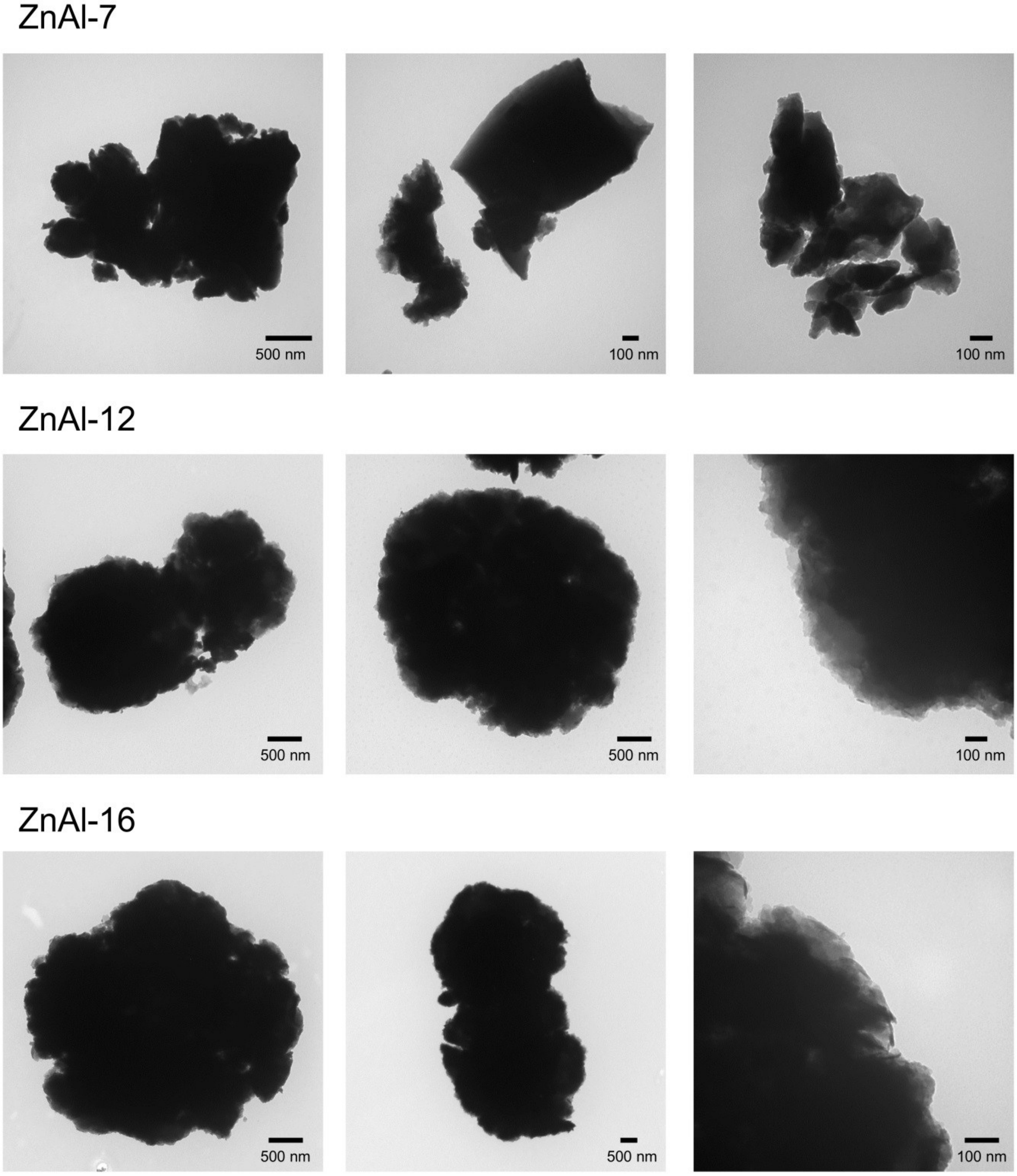

Figure S2a: Additional TEM images of ZnAl-7, ZnAl-12, and ZnAl-16 illustrating the changes in particle morphology from seven to 16 h of reaction time.

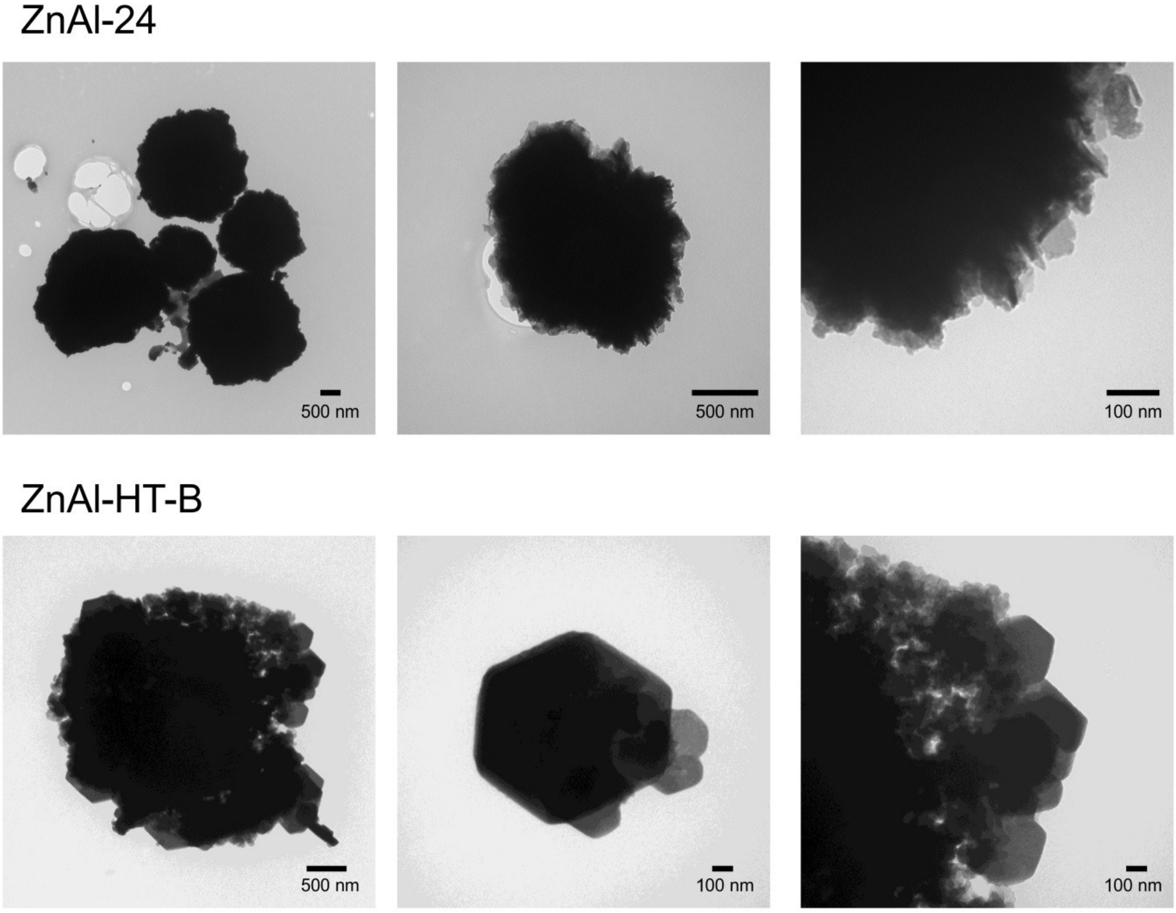

Figure S2b: TEM images of the samples ZnAl-24 (as synthesized) and the hydrothermally treated sample ZnAl-HT-B.

Experimental details of the bentonite ion-exchange experiment:

50 mL of the reaction mixture was collected after a reaction time of 3, 4, 5, and 6 h, respectively, and rapidly cooled to room temperature by placing the reactor in cold water. Subsequently, 0.1 g of Na-bentonite (Sigma-Aldrich) was added and the suspension stirred for 24 h to facilitate cation exchange under a nitrogen flow. The pH at the end of the reaction was: 3.5(1), 4.0(1), 4.6(1), and 5.3(1) after 3, 4, 5, and 6 h, respectively. The solid product was washed and isolated by centrifugation using the same procedure as for the LDHs. Subsequently, a suspension of the product was formed by addition of a small amount of water. Samples for PXRD were oriented along the *c*-axis by addition of a few drops of the suspension to a PXRD sample holder. The sample was air dried prior to PXRD measurements.

PXRD of the samples from the bentonite ion-exchange experiment

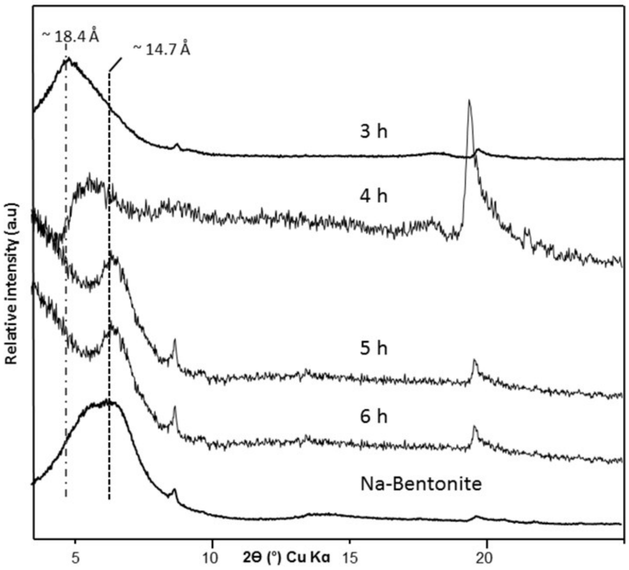

Figure S3: PXRD of the bentonite ion-exchanged samples and the sodium bentonite reactant(Na-Bentonite), which has a d-spacing of 14.7 Å. This value is slightly larger due to swelling than reported for dried bentonite.[2, 3] At 3 h the bentonite d-spacing is 18.4 Å indicating intercalation of the Al_{13} Keggin ion, $[AlO_4Al_{12}(OH)_{24}(H_2O)_{12}]^{7+}$,[2, 4] which is only stable in the pH-region below 4-5.[5, 6] However, at longer reaction times (5 and 6 h) no change in d-spacing is observed.

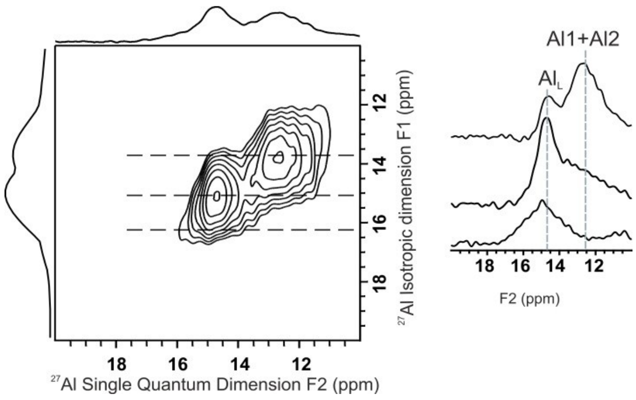

Figure S4: The region for octahedral Al in the ^{27}Al 3QMAS NMR spectra of ZnAl-24 recorded at 22.3 T. The ^{27}Al 3QMAS NMR spectra were obtained from the three pulse sequence with z-filter,[7] referenced according to Amoureux,[8, 9] with a recycle delay of 4 s.

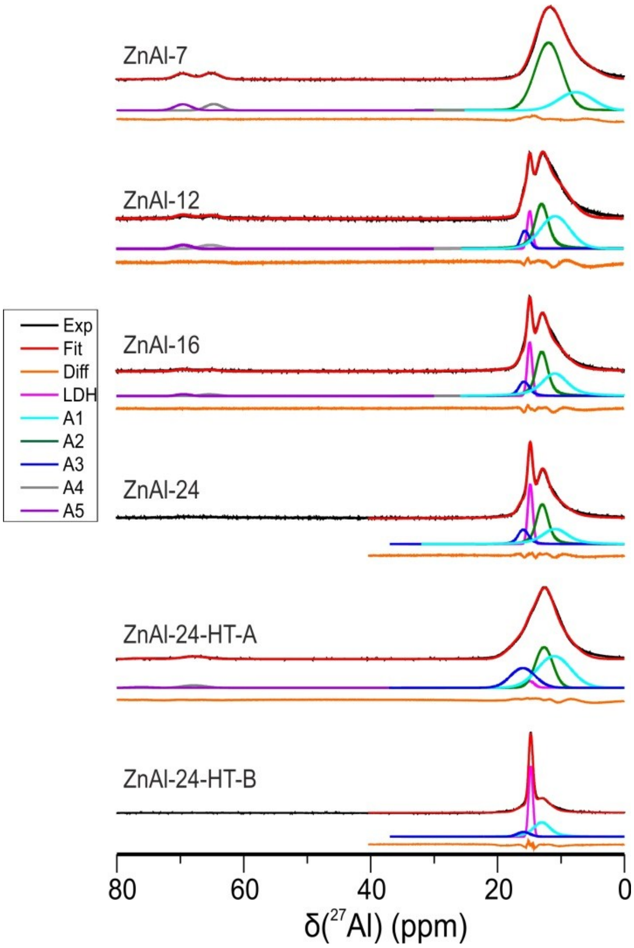

Figure S5: Deconvolution of the ^{27}Al MAS NMR spectra (22.3 T, 35 kHz spinning). Parameters used for the deconvolution are given in Table S3. For ZnAl-24 and ZnAl-HT-B only the octahedral region of the ^{27}Al MAS NMR spectrum was analyzed, as the intensities from tetrahedral Al species were negligible.

Table S3: Isotropic chemical shift ($\delta_{iso}(^{27}Al)$), quadrupolar effect parameter (P_Q), quadrupolar coupling constant (C_Q), asymmetry parameter (η_Q) and relative intensity (I) for each site determined from ^{27}Al 3QMAS and single pulse ^{27}Al MAS NMR spectra recorded at 22.3 T with 35 kHz Spinning (NA – not applied).

		^{27}Al 3QMAS		**^{27}Al single pulse deconvolution**				
Sample	**Site**	**δ_{iso} (^{27}Al) (ppm)**	**P_Q (MHz)**	**$\delta_{iso}(^{27}Al)$ (ppm)**	**Width (Hz)**	**C_Q (MHz)**	**η_Q**	**I (%)**
ZnAl-7	A1	-	-	8.5(5)	1550	2.8(2)	0.4(3)	24(4)
	A2	13.09(1)	3.48(1)	12.8	1200	3.4(2)	0.2(2)	68(5)
	A4	66.11(6)	2.92	65.9(1)	700	3.0(1)	0.0(1)	4(2)
	A5	70.91(4)	(15) 3.49(15)	70.4(1)	700	3.0(1)	0.0(1)	4(2)
ZnAl-12	A_L	14.95(2)	1.46(8)	15.1(1)	210	1.5(1)	0.0(1)	8(2)
	A1	-	-	11.7(1)	1400	3.0(1)	0.4(3)	45(4)
	A2	13.58(2)	3.26(2)	13.8(1)	650	2.8(2)	0.2(4)	34(4)
	A3	-	-	16.4(1)	280	2.8(2)	0.2(2)	7(2)
	A4	-	-	66.0(1)	800	3.0(1)	0.0(1)	3(2)
	A5	-	-	70.3(1)	700	3.0(1)	0.0(1)	3(2)
ZnAl-16	A_L	14.95(2)	1.66(1)	15.1(1)	210	1.5(1)	0.0(1)	14(2)
	A1	11.40(1)	2.86(1)	11.8(1)	1400	3.0(2)	0.4(3)	39(7)
	A2	13.50(1)	3.08(2)	13.8(1)	550	2.8(2)	0.2(4)	34(2)
	A3	-	-	16.6(1)	450	3.0(1)	0.3(3)	10(5)
	A4	-	-	66.2(1)	700	3.0(2)	0.0(1)	1(1)
	A5	-	-	70.3(1)	600	3.0(2)	0.0(1)	2(1)
ZnAl-24	A_L	14.86(2)	1.51(8)	15.1(1)	210	1.5(1)	0.0(1)	21(3)
	A1	-	-	11.8(1)	1300	3.0(1)	0.4(3)	33(4)
	A2	13.27(2)	2.87(2)	13.8(1)	550	2.8(2)	0.2(4)	34(4)
	A3	-	-	16.8(1)	450	3.0(1)	0.3(3)	12(3)
ZnAl-HT-B	A_L	NA	NA	15.0(1)	185	1.5(1)	0.0(1)	45(4)
	A2			13.9(1)	900	2.8(1)	0.2(2)	47(4)
	A3			16.8(1)	500	3.0(1)	0.5(2)	8(2)

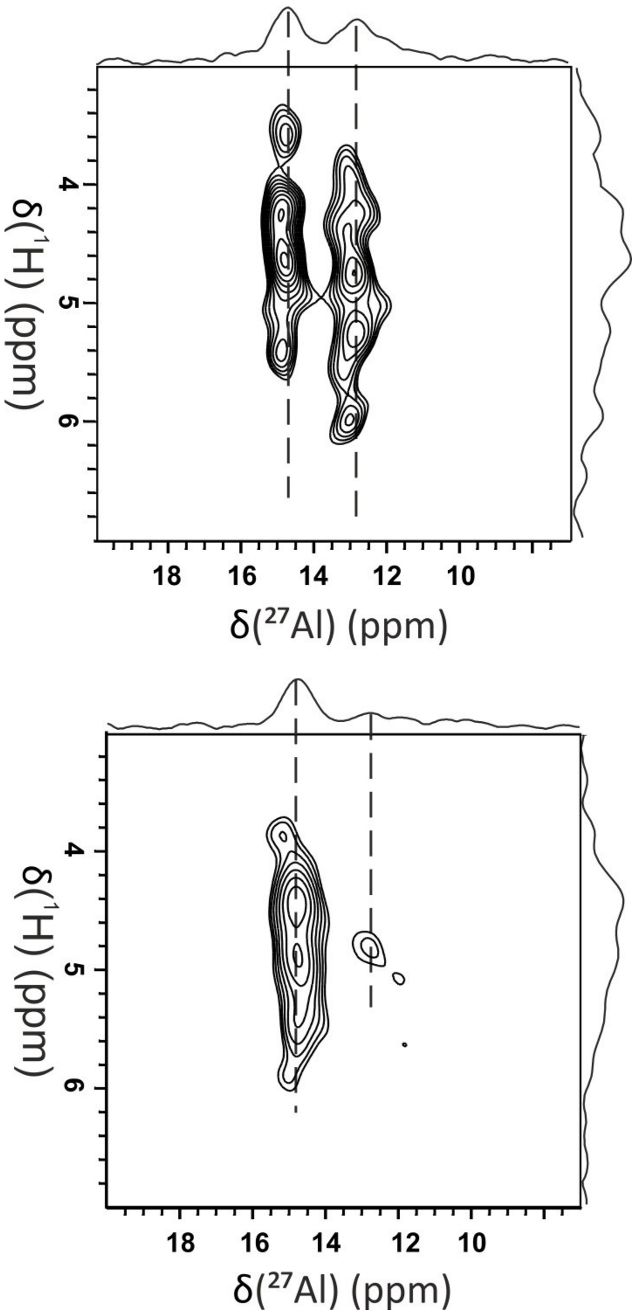

Figure S6: ^{27}Al{^{1}H} HETCOR NMR of a) ZnAl-24 and b) ZnAl-HT-B illustrating the effect of hydrothermal treatment of the isolated product using a 100 μs contact time.

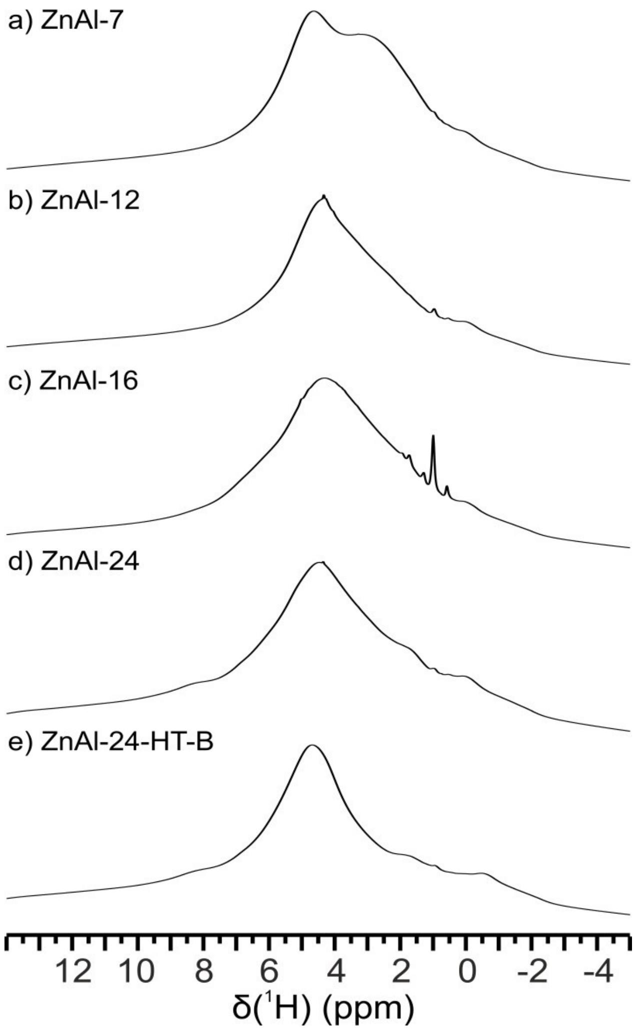

Figure S7: ^{1}H MAS NMR spectra collected at 22.3 T using 35 kHz spinning speed.

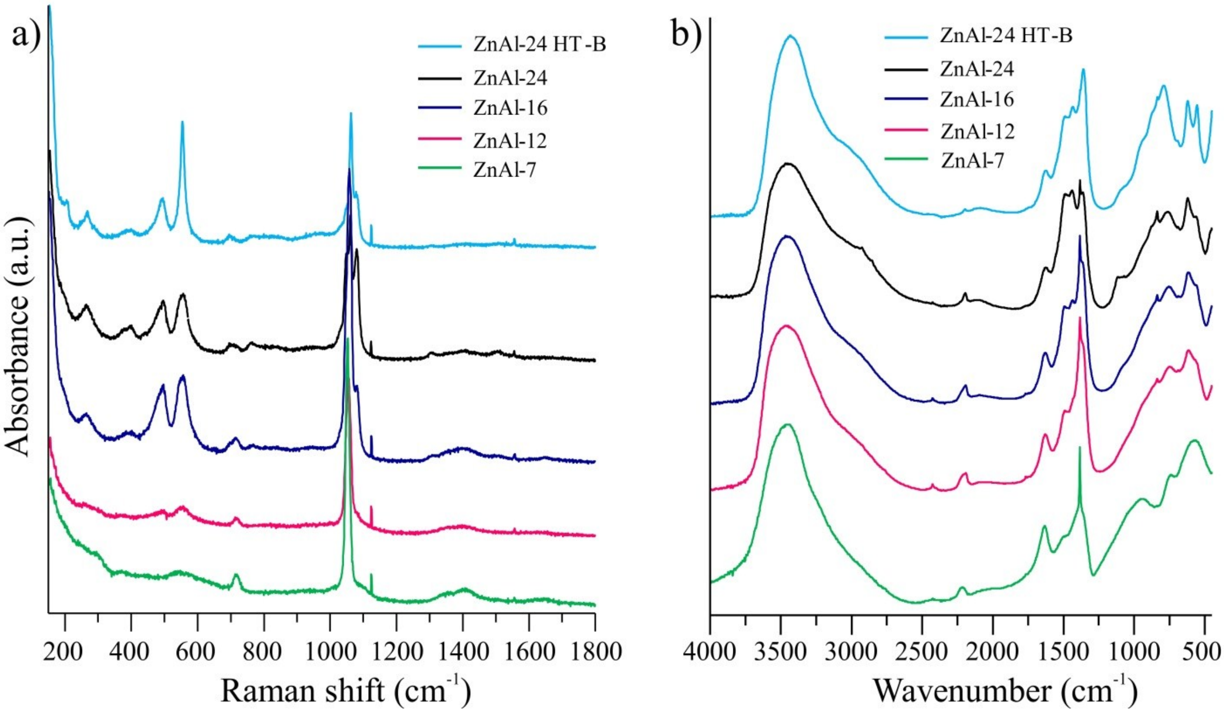

Figure S8: a) Raman and b) infrared spectra of the ZnAl-X series.

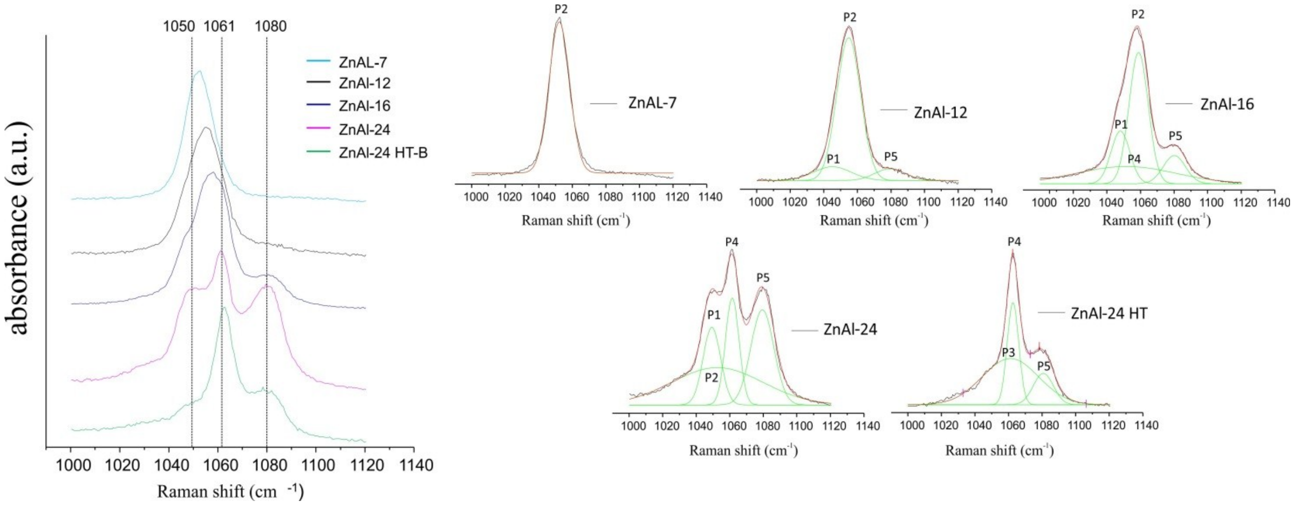

Figure S9: Deconvolution of the Raman vibration bands in the 1000-1120 cm^{-1} spectral region for the ZnAl-X series.

Table S4: Peak assignments of the Raman spectra for the ZnAl-X series in the 1000-1120 cm^{-1} spectral region (Figure S10) with the goodness of the fitted spectrum (r^2).

Peak (cm^{-1})	**ZnAl-7**	**ZnAl-12**	**ZnAL-16**	**ZnAl-24**	**ZnAl-24 HT**	**Assignment**
Peak 1		1045	1048	1049		
Peak 2	1052	1055	1051	1052		
Peak 3					1061	$\nu_1(CO_3)$
Peak 4			1059	1061	1063	$\nu_1(CO_3)$
Peak 5		1080	1080	1079	1080	$\nu_1(NO_3)$
r^2	0.995	0.9988	0.9986	0.997	0.9975	

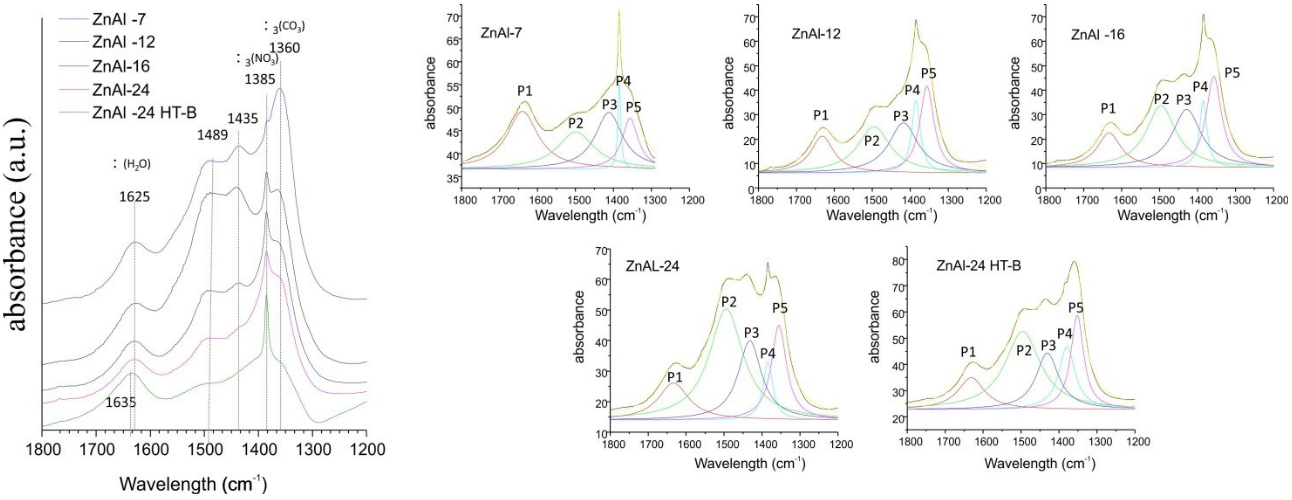

Figure S10: Deconvolution of the Raman vibration bands in the 1200-1800 cm^{-1} spectral region for the ZnAl-X series.

Table S5: Peak assignments for FT-IR spectra of the ZnAl-X series in the 1200-1800 cm^{-1} spectral region (Figure S11).

Peak (cm^{-1})	**ZnAl-7**	**ZnAl-12**	**ZnAL-16**	**ZnAl-24**	**ZnAl-24 HT**	**Assignment**
Peak 1	1640	1632	1632	1633	1631	$\delta(H_2O)$
Peak 2	1499	1496	1496	1494	1496	
Peak 3	1412	1418	1428	1432	1431	$\delta(NH_4^+)$
Peak 4	1385	1385	1385	1384	1379	$\nu_3(NO_3$
Peak 5	1356	1356	1357	1355	1352	$\nu_3(CO_3)$
r^2	0.9941	0.9975	0.9985	0.9986	0.9986	

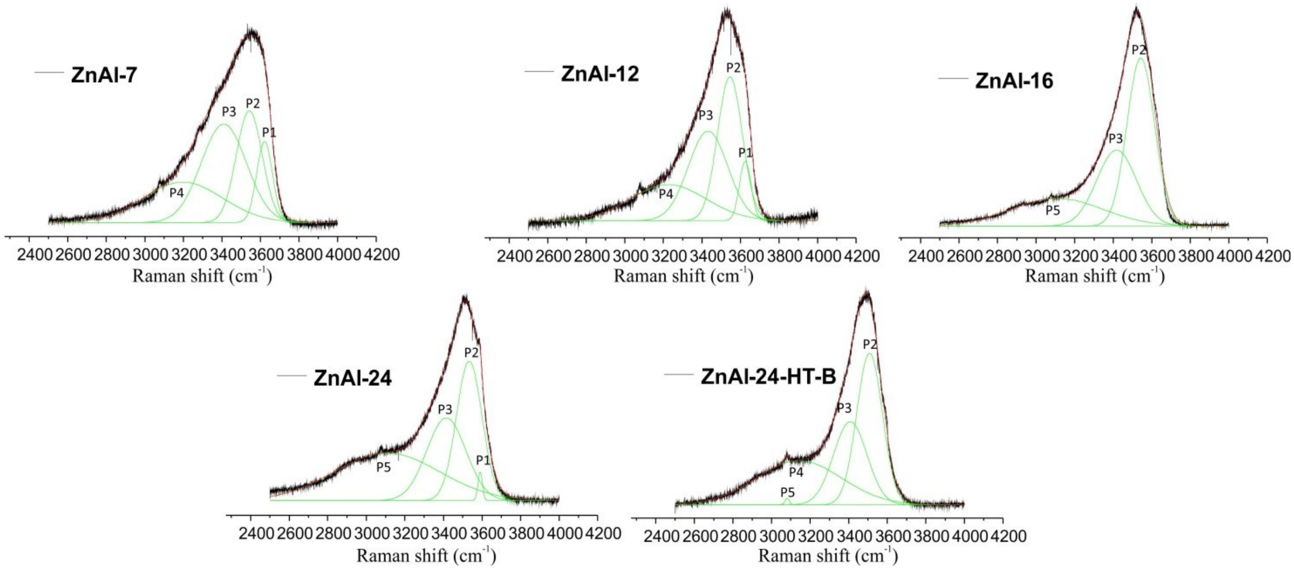

Figure S11: Deconvolution of the MO-H and HO-H Raman vibration bands in the 2500-4000 cm^{-1} spectral region for the ZnAl-X series.

Table S6: Peak assignments for FT-IR spectra of the ZnAl-X series in the 2500 -4000 cm^{-1} spectral region (Figure S12).

Peak (cm^{-1})	**ZnAl-7**	**ZnAl-12**	**ZnAl-16**	**ZnAl-24**	**ZnAl-24-HT**
Peak 1	3621	3625		3590	
Peak 2	3543	3546	3543	3534	3508
Peak 3	3411	3432	3418	3415	3408
Peak 4	3198	3226			3143
Peak 5			3109	3107	3080
r^2	0.9979	0.9975	0.9968	0.9979	0.9984

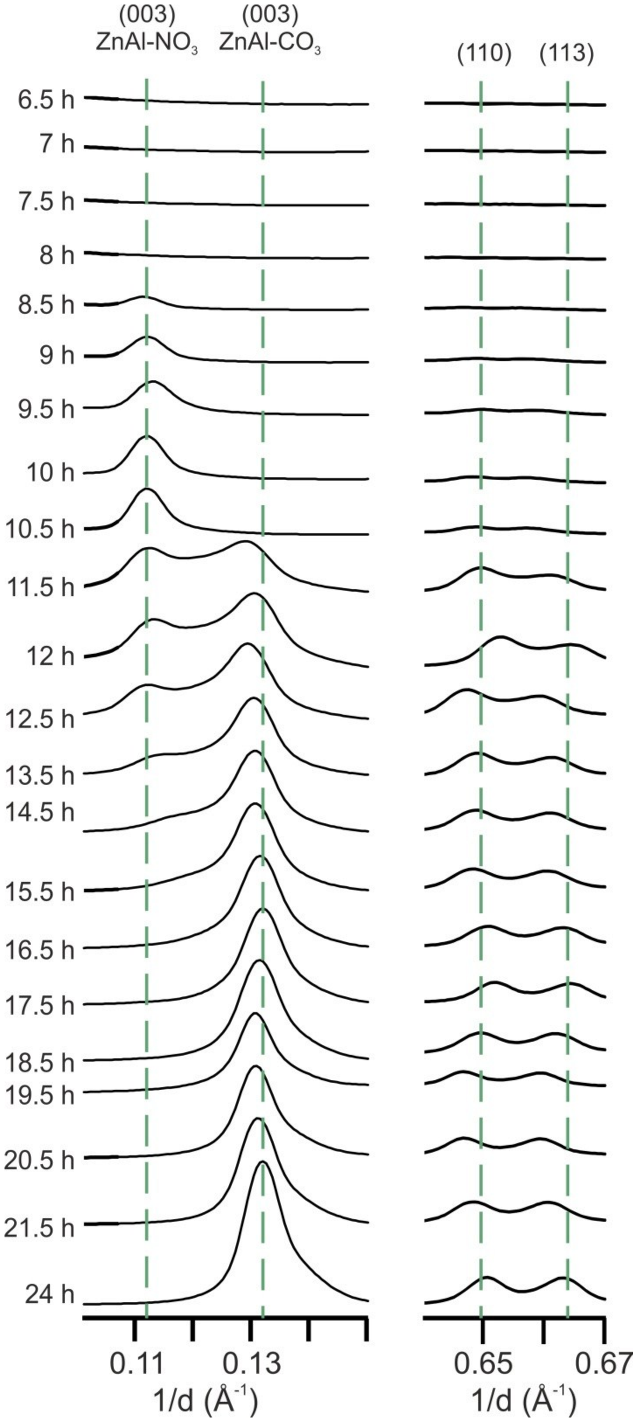

Figure S12: Expansion of the (003), (110), and (113) reflections in the PXRD diffractograms (Figure 10) for the time resolved study. The anion (nitrate vs carbonate) and average metal-to-metal distances are identified by the position of the (003) and (110) reflections, respectively.

References

1. S. S. C. Pushparaj, C. Forano, V. Prevot, A. S. Lipton, G. J. Rees, J. V. Hanna and U. G. Nielsen, *J. Phys. Chem. C*, 2015, **119**, 27695-27707.
2. A. Gil, A. Diaz, M. Montes and D. R. Acosta, *J.Mater.Sci.*, 1994, **29**, 4927-4932.
3. M. E. R. Jalil, R. S. Vieira, D. Azevedo, M. Baschini and K. Sapag, *Appl. Clay Sci.*, 2013, **71**, 55-63.
4. F. Bergaya, A. Aouad and T. Mandalia, in *Developments in Clay Science*, eds. B. K. G. T. Faïza Bergaya and L. Gerhard, Elsevier, 2006, vol. Volume 1, pp. 393-421.
5. C. H. Feng, Q. S. Wei, S. F. Wang, B. Y. Shi and H. X. Tang, *Colloids Surf. a-Physicochemical and Engineering Aspects*, 2007, **303**, 241-248.
6. A. Etou, S. Q. Bai, T. Saito, H. Noma, Y. Okaue and T. Yokoyama, *J. Colloid and Interface Sci.*, 2009, **337**, 606-609.
7. J. P. Amoureux, C. Fernandez and S. Steuernagel, *J. Magn. Reson. Ser. A*, 1996, **123**, 116-118.
8. J. P. Amoureux and C. Fernandez, *Solid State Nucl.Magn. Reson.*, 2000, **16**, 339-343.
9. J. P. Amoureux and C. Fernandez, *Solid State Nucl. Magn. Reson.*, 1998, **10**, 211-223.